THE ROYAL SOCIETY

doi 10.1098/rspb.2001.1663

Anomalous mole-fraction effects in recombinant and native cyclic nucleotide-gated channels in rat olfactory receptor neurons

W. Qu[1], A. J. Moorhouse[1], A. M. Cunningham[2,3] and P. H. Barry[1*]

[1]*Schools of Physiology and Pharmacology, and* [2]*Paediatrics, The University of New South Wales, Sydney 2052, Australia*
[3]*Neurobiology Division, Garvan Institute of Medical Research, Darlinghurst, Sydney 2010, Australia*

Anomalous mole-fraction effects (AMFE) were studied, using the inside-out configuration of the patch-clamp technique, in both recombinant wild-type α-homomeric rat olfactory adenosine 3′,5′-cyclic monophosphate (cAMP)-gated channels (rOCNCl) expressed in human embryonic kidney cells (HEK 293) and native cyclic nucleotide-gated (CNG) channels in acutely isolated rat olfactory receptor neurons. Single-channel and macroscopic currents were activated by 200 μM and 500 μM cAMP, respectively. Macroscopic currents, measured with mixtures of Na^+–NH_4^+ or Cs^+–Li^+ in the cytoplasmic bathing solution, displayed AMFE in the rOCNCl channels at both positive and negative membrane potentials. The rOCNCl single-channel conductance showed a distinct minimum (or maximum) in an 80% Na^+–20% NH_4^+ mixture (or a 60% Cs^+–40% Li^+ mixture), but only at positive membrane potentials. Macroscopic measurements in native olfactory CNG channels with mixtures of Na^+–NH_4^+ indicated similar AMFE. These results suggest that both native CNG channels and recombinant α-homomeric channels allow several ions to be present simultaneously within the channel pore. They also further validate the dominant role of the α-subunit in permeation through these channels, provide the first evidence to suggest that rOCNCl channels have multi-ion properties and further justify the use of the rOCNCl channel as an effective model for structure–function studies of ion permeation and selectivity in olfactory CNG channels.

Keywords: anomalous mole-fraction effects; cyclic nucleotide-gated channels; patch clamp; cyclic AMP; olfactory receptor neurons; rOCNCl

1. INTRODUCTION

Olfactory cyclic nucleotide-gated (CNG) channels play a crucial role in the conversion of an odour-induced chemical change into an electrical signal. The CNG channel is a tetrameric complex, composed of distinct, but highly homologous, α- and β-subunits (e.g. Zagotta & Siegelbaum 1996). The α-subunit is able to homomerically form a functional channel, but the properties of α-homomeric recombinant channels have been shown to differ from those of the native CNG channels in both ligand sensitivity and gating (Bradley *et al*. 1994). However, the cation-permeation properties of recombinant and native channels are generally similar (Qu *et al*. 2000). Thus, the recombinant channel provides a good model for exploring the mechanism of permeation through CNG channels, at the molecular level, the details of which remain uncertain. An important issue in understanding the molecular basis of ionic permeation through these channels is to establish whether they behave as simple single-ion pores or as multi-ion pores, occupied concurrently by more than one ion. One of the classical tests to determine the multi-ion nature of a pore is to establish the presence or absence of anomalous mole-fraction effects (AMFE) (e.g. Hagiwara *et al*. 1977; Hille 1992).

AMFE are thought to originate from interactions between permeant ions of the same or different species within the channel pore (Almers & McCleskey 1984). The experimental procedure involves holding constant the sum of the concentrations of two different species of permeating ions in the appropriate bathing solution, while the ratio of their concentrations (or mole fraction) is changed. The effects are referred to as 'anomalous' because the permeation parameter (e.g. reversal potential, V_{rev}, or single-channel conductance, γ) deviates from its expected monotonic dependence on the mole fraction. Instead, the parameter may pass through a distinct minimum or maximum relative to its value in either of the two equimolar pure symmetrical solutions, as the mole fraction is changed. AMFE in channels indicate a deviation from a simple one-site ion-binding model and can be explained by a multi-ion model in which two or more ions simultaneously exist and interact in the channel pore (e.g. Hagiwara *et al*. 1977; Hille & Schwarz 1978; see also reviews in Hille 1992 and Lester & Dougherty 1998).

For CNG channels, some controversy exists with regard to AMFE. No AMFE were observed in native rod guanosine 3′,5′-cyclic monophosphate (cGMP)-gated channels in Na^+–Li^+ (Menini 1990) or Na^+–Ca^{2+} mixtures (e.g. Zimmerman & Baylor 1992). Nor was AMFE found in the presence of Na^+–Li^+ mixtures in native adenosine 3′,5′-cyclic monophosphate (cAMP)-gated channels in frog olfactory receptor neurons (ORNs) (Frings *et al*. 1992). However, using other pairs of ions in native rod CNG channels, AMFE have been reported for reversal potentials in the presence of NH_4^+–Na^+, and Cs^+–Na^+, mixtures (Furman & Tanaka 1990), Na^+–Ca^{2+} mixtures in the presence of triphosphate nucleotides

*Author for correspondence (p.barry@unsw.edu.au).

(Rispoli & Detwiler 1990) and Li^+–Cs^+ mixtures (Sesti *et al*. 1995). Sesti *et al*. (1995) also suggested that the molecular basis for multi-ion interactions in recombinant cGMP-gated channels involved the negative glutamate 363 residue in its putative pore region, since AMFE were absent when this residue was mutated to glutamine or aspartate.

An alternative explanation suggested for AMFE, which does not involve ion interactions in the pore, is that one of the ionic species binds to an external site to modify channel gating or permeation (e.g. Hille & Schwarz 1978). The possibility that AMFE are due to an external regulatory site that affects the gating of a particular ionic channel is readily testable by measuring either changes in reversal potential or relative permeability, or changes in single-channel conductance, as a function of mole fraction. Both of these sets of measurements would be expected to be independent of gating. In the unlikely event that a putative external regulatory site also selectively affected the permeation properties of an ion, these criteria would not distinguish between this model and that of multi-ion occupancy. However, we would not expect an external-site model to be very voltage sensitive. Provided that the AMFE behaviour is due to an interaction between ions within an ion channel, the presence of such effects between any pair of ions should be sufficient to indicate multiple-ion occupancy of the channel. The effect relies on induced effects between ions of different species and is expected to be greater for certain pairs of ions, particularly when one of them is large and polarizable (Hille & Schwarz 1978).

In order to investigate the hypothesis of multi-ion occupancy of rat olfactory CNG channels, we conducted a series of recordings in the α-homomeric CNG channels at both the macroscopic and single-channel levels, together with some recordings in native olfactory CNG channels, and compared the results from both preparations. We tested two pairs of cations, Na^+–NH_4^+, and Cs^+–Li^+, in various mixtures in inside-out patches.

2. MATERIAL AND METHODS

(a) *Preparation of rat ORNs*

Adult female Wistar rats (body weight, 130–150 g) were killed and decapitated after inhaling carbon dioxide for *ca*. 2–3 min. The olfactory epithelium was enzymatically digested by incubation in a general mammalian Ringer's solution (see §2(c)) containing 0.022% trypsin at 37 °C for *ca*. 28 min (for further details see Lynch & Barry 1989). The suspension was gently triturated with a wide-bore Pasteur pipette and the supernatant, which contained dissociated ORNs, was then transferred to the recording chamber with an uncoated glass base, which was kept at room temperature; the cells could be used for up to *ca*. 8 h.

(b) *Expression of rat rOCNC1 CNG channel cDNAs in HEK 293 cells*

Plasmid cDNA encoding the wild-type α-subunit of the rat olfactory cyclic-nucleotide-activated channel (rOCNC1 (Dhallan *et al*. 1990) alternatively designated CNG2) subcloned in the vector pCIS2 was transiently transfected into exponentially growing HEK 293 cells using the Ca-phosphate precipitate method (Chen & Okayama 1987). After transfection for 24 h, the cells were washed twice and placed in fresh Eagle's minimum essential medium in Hanks' salts (Trace Scientific, Melbourne, Australia), supplemented with 2 mM glutamine and 10% foetal calf serum. Transfected cells were grown on glass cover-slips, coated with collagen and poly-D-lysine, and used within 72 h. The CD4 surface antigen cDNA was co-expressed so that the transfected HEK 293 cells could be identified by labelling them with CD4 antibody-coated polystyrene beads (Dynabeads M-450, Dynal A.S., Oslo, Norway).

(c) *Electrophysiology*

Macroscopic currents, where the average current from a considerable number of channels could be recorded, and single-channel cAMP-gated currents were activated by 500 μM and 200 μM cAMP, respectively, in inside-out patches excised from HEK 293 cells expressing rOCNC1 channels. Between recordings, cells were continuously perfused with a general mammalian Ringer's bath solution containing 140 mM NaCl, 5 mM KCl, 2 mM $CaCl_2$, 2 mM $MgCl_2$, 10 mM N-[2-hydroxyethyl]-piperazine-N′-[2-ethanesulphonic acid] (HEPES) and 10 mM glucose; the pH was adjusted to 7.4 with 1 M NaOH. All experiments were performed at room temperature (20–22 °C). Upon excision of the patch, the internal surface was perfused with a bath solution comprising a range of test solutions to look for AMFE. For the Na^+–NH_4^+ mixtures, for Na^+mole fractions ($X_{Na} = [Na^+]/([Na^+] + [NH_4^+])$ of 1, 0.8, 0.6, 0.4, 0.2 and 0, the concentrations of $[Na^+]$ were 149 mM, 120 mM, 91 mM, 62 mM, 33 mM and 4 mM, respectively, and of $[NH_4^+]$ were 0 mM, 29 mM, 58 mM, 87 mM, 116 mM and 145 mM, respectively. For the Cs^+–Li^+ mixtures, for Cs^+ mole fractions ($X_{Cs} = [Cs^+]/([Cs^+] + [Li^+])$ of 1, 0.8, 0.6, 0.4, 0.2 and 0, the concentrations of $[Cs^+]$ were 145 mM, 116 mM, 87 mM, 58 mM, 29 mM and 0 mM, respectively, and of $[Li^+]$ were 0 mM, 29 mM, 58 mM, 87 mM, 116 mM and 145 mM, respectively. In each test solution, the concentrations of $[Cl^-]$ and HEPES were 145 mM and 10 mM, respectively, and the pH was adjusted to 7.4 with 1 M NaOH. For the Na^+–NH_4^+ experiments, the patch electrodes were filled with a solution of 145 mM NaCl and 10 mM HEPES, while for the Cs^+–Li^+ experiments, NaCl was replaced by CsCl. For both sets of experiments, the pH was adjusted to 7.4 with 1 M NaOH. Test solutions were delivered by gravity from a set of parallel polyethylene tubes and solution changes were made by moving pipettes with attached patches from one perfusion tube to the next (for further experimental details see Qu *et al*. 2000). During the experiments, the mole fractions (X_{Na} and X_{Cs}) were sequentially varied from 1.0 to 0.

Pipette resistances for macroscopic and single-channel recordings in HEK 293 cells were 8–10 MΩ and 15–18 MΩ, respectively. For rat ORNs, macroscopic currents were obtained with pipettes having resistances of 12–15 MΩ. The voltage-clamp amplifier was an Axopatch 1D (Axon Instruments, Union City, CA) with a Digidata 1200 (Axon Instruments, Union City, CA) connected to a 166 MHz Pentium computer. Voltage control, data acquisition and data analyses were performed using pClamp 8.0 (Axon Instruments, Union City, CA) and Sigmaplot 5.0 (SPSS Inc, Chicago, IL). Both single-channel and macroscopic data were filtered at 2 kHz and sampled at 10 kHz. Macroscopic currents were recorded for a series of voltage pulses of 500 ms duration, stepping the voltage from the holding potential of 0 mV to different command potentials ranging from −60 mV to +80 mV, at intervals of 10 mV. Single-channel recordings were measured at holding potentials from −60 mV to +60 mV for durations of 30 s.

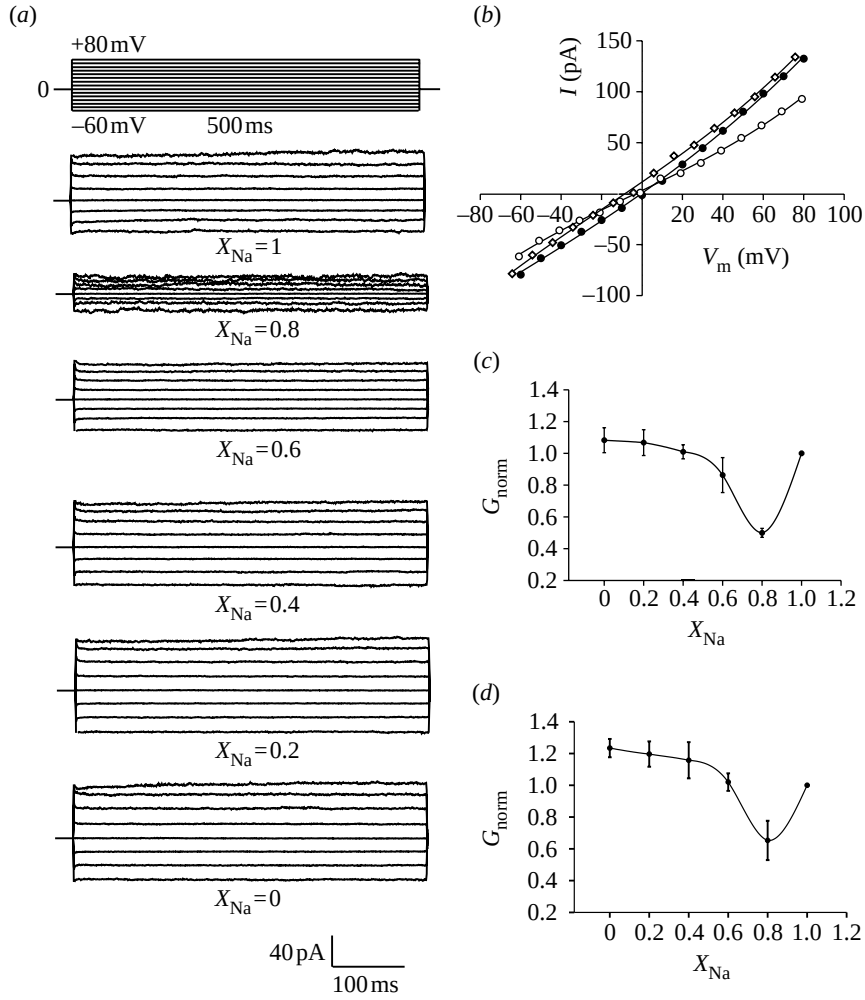

Figure 1. Macroscopic currents through rOCNC1 channels in Na^+–NH_4^+ mixtures display anomalous mole-fraction effects. (*a*) Representative macroscopic currents in one inside-out patch with different mole fractions of Na^+ ($X_{Na} = [Na^+]/\{[Na^+] + [NH_4^+]\}$) in the intracellular solution. The top panel shows the pulse protocol and lower panels display every second trace. The small bar to the left of each set of traces indicates the zero-voltage trace. (*b*) *I–V* curves in one patch with decreasing X_{Na} on the cytoplasmic side ($X_{Na} = 1$ (filled circles), $X_{Na} = 0.8$ (empty circles) and $X_{Na} = 0$ (open diamonds)). Lines are least-square polynomial fits. The currents went through a distinct minimum at $X_{Na} = 0.8$ for both positive and negative membrane potentials. Normalized mean chord conductance curves between (*c*) +60 mV ($n = 4$) and the reversal potential (V_{rev}) and (*d*) V_{rev} and −60 mV ($n = 4$) plotted against X_{Na}. Error bars show s.e.m.

For all experiments, membrane potentials are reported with respect to the external membrane surfaces and have been corrected for liquid-junction potentials using the Windows version of the JPCalc program (Barry 1994). Macroscopic current amplitude was determined as the difference between current recordings in the presence and absence of cAMP. The single-channel current amplitudes for different mixtures of cations were calculated from an amplitude-histogram analysis fitted with two Gaussian distributions. The mean reversal potential, V_{rev}, in each case was obtained from an interpolation of the corresponding current–voltage curves. Both reversal potentials and normalized chord conductances were measured for different mole fractions of test cations. The macroscopic chord conductances (G) at different membrane potentials (V_m) were calculated by dividing the current amplitudes (I) by the difference between V_m and the corresponding V_{rev}: $G = I/(V_m - V_{rev})$. The mean normalized value, G_{norm}, was calculated by dividing G by its value in the 'pure' $[Na^+]$ solution and averaging the data for all patches used. Single-channel conductances, γ and γ_{norm} were equivalently defined. Data are expressed as mean ± s.e.m. and statistical analyses were performed using the Student's paired *t*-test.

3. RESULTS

(a) *Anomalous mole-fraction experiments in rOCNC1 channels*

In order to investigate the pore properties of recombinant olfactory CNG channels, we assessed the effects of different combinations of Na^+ and NH_4^+ perfusing the intracellular side of the membrane, while holding their total concentration constant and varying the mole fraction, X_{Na}, sequentially from 1.0 to 0. With 100% of either Na^+ or NH_4^+, the macroscopic currents were quite large, confirming that both cations were highly permeable through the channel (figure 1*a*; see also Qu *et al.* 2000). The mean reversal potentials (V_{rev}) (figure 1*b*) were -9.0 ± 0.4 mV ($X_{Na} = 0$), -5.5 ± 1.2 mV ($X_{Na} = 0.8$) and 0.5 ± 0.5 mV ($X_{Na} = 1.0$) ($n = 4$), showing no AMFE. When $X_{Na} = 0.8$, however, the macroscopic currents were

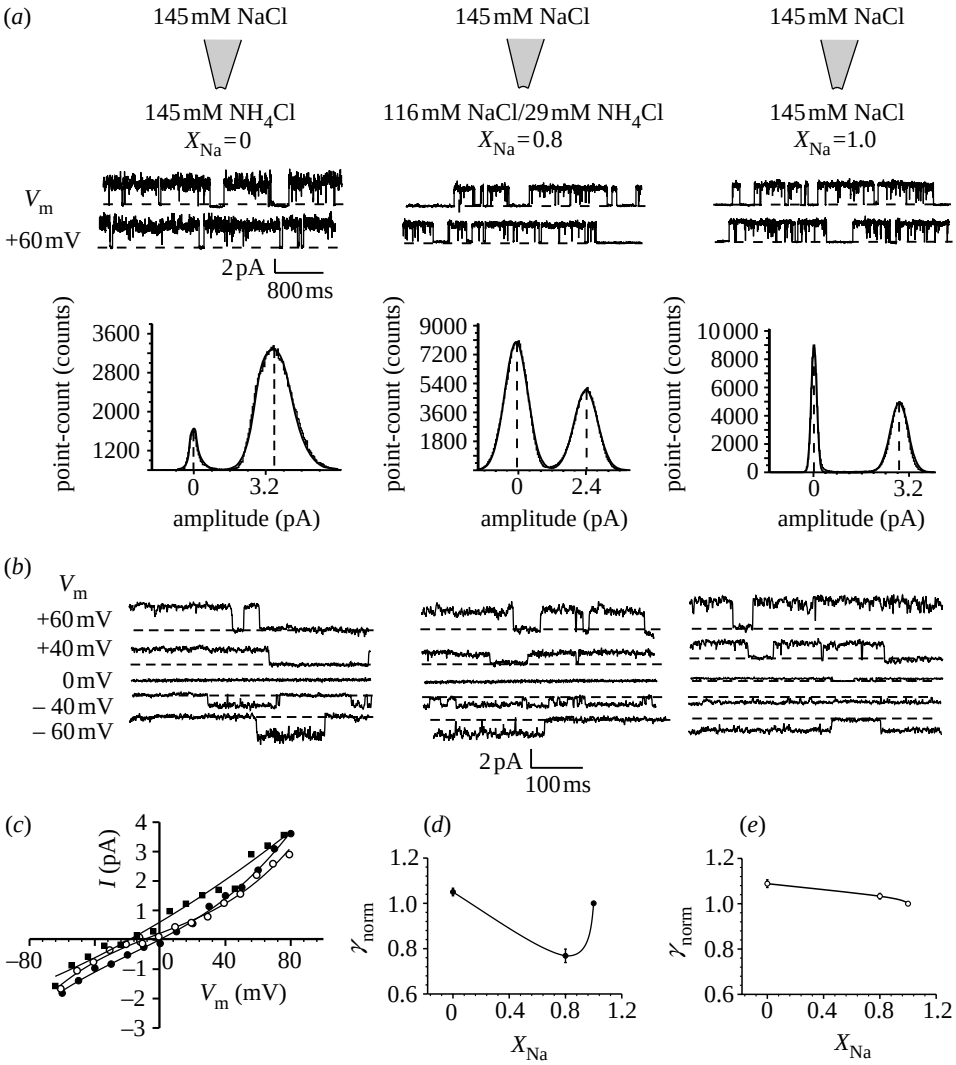

Figure 2. Single-channel properties of rOCNC1 channels for inside-out patches bathed in cytoplasmic Na^+–NH_4^+ mixtures elicited by 200 μM cAMP. Pipettes contained 145 mM NaCl. (*a*) The upper panel shows parts of 30 s current traces for $X_{Na}=0$, 0.8 and 1.0 at a membrane potential, V_m, of +60 mV, where $X_{Na}=[Na^+]/([Na^+]+[NH_4^+])$. Corresponding amplitude histograms are shown in the lower panels, fitted with the sum of two Gaussian distributions; mean values are shown as dashed vertical lines. Note the decrease in open probability for $X_{Na}=0.8$. The estimated mean current amplitudes for this patch in the three solutions were 3.6 pA ($X_{Na}=0$), 2.4 pA ($X_{Na}=0.8$) and 2.8 pA ($X_{Na}=1.0$). (*b*) Parts of representative 1.5 s single-channel traces at several membrane potentials in one inside-out patch with $X_{Na}=0$ (left), 0.8 (middle) and 1.0 (right). Dashed lines show the closed-channel current level. (*c*) Current–voltage (*I*–*V*) curves for $X_{Na}=0$ (filled squares), $X_{Na}=0.8$ (empty circles) and $X_{Na}=1$ (filled circles) in another patch. Normalized mean chord conductances at membrane potentials of (*d*) +60 mV and (*e*) −60 mV ($n=3$). AMFE are clearly displayed at $V_m=+60$ mV but not at $V_m=-60$ mV. Error bars indicate s.e.m.

smaller than those observed in the presence of either species by itself, and this occurred at both positive and negative potentials (figure 1*c*,*d*). The corresponding mean normalized chord conductances for four patches between +60 mV and V_{rev} were 1.08 ± 0.08 ($X_{Na}=0$), 0.50 ± 0.03 ($X_{Na}=0.8$) and 1.0 ($X_{Na}=1.0$), while the mean normalized chord conductances between V_{rev} and −60 mV in the same four patches were 1.2 ± 0.06 ($X_{Na}=0$), 0.7 ± 0.12 ($X_{Na}=0.8$) and 1.0 ($X_{Na}=1.0$). These results indicate that macroscopic rOCNC1-channel currents in HEK 293 cells went through a minimum at a mole fraction of *ca.* 0.8 at both +60 mV and −60 mV. Hence, in these solutions, rOCNC1 channels exhibited AMFE without any voltage dependence.

We also studied the effect of mixtures of these two cations at the single-channel-current level. Single-channel currents were elicited by 200 μM cAMP and recorded at different membrane potentials for 30 s at each potential. In accordance with the results from the macroscopic recordings, conductance was measured in Na^+–NH_4^+ solution mixtures for $X_{Na}=0$, 0.8 and 1. Representative single-channel currents measured in one patch in these three solutions at five membrane potentials are shown in figure 2*b*. The single-channel current amplitudes from individual patches under the three ionic conditions were obtained by fitting all point-amplitude histograms with the sum of two Gaussian distributions for the closed- and open-channel current levels, respectively (figure 2*a*). The *I*–*V* curves measured in these three solutions (figure 2*c*) suggest that at membrane potentials more positive than about +20 mV the current recorded in the Na^+–NH_4^+ mixed solution is less than that recorded in either

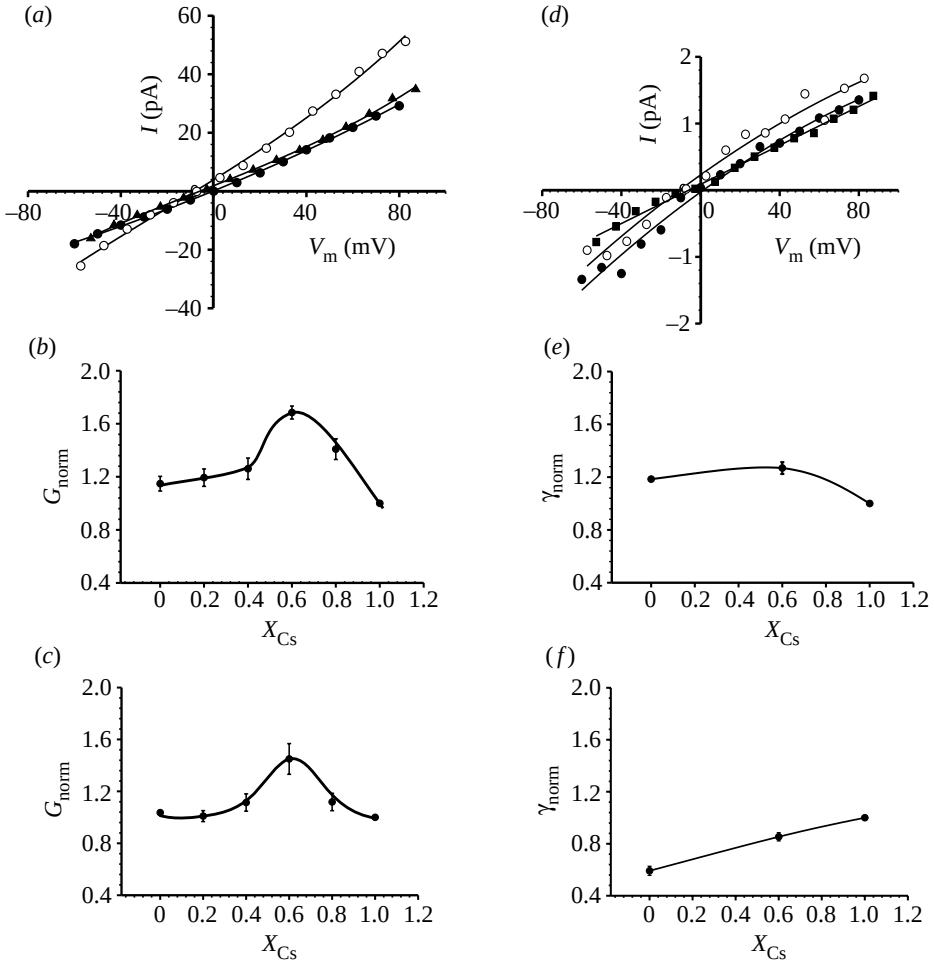

Figure 3. (*a–c*) Macroscopic and (*d–f*) single-channel currents recorded in rOCNC1 channels in cytoplasmic Cs^+–Li^+ mixtures (mole fraction, $X_{Cs} = [Cs^+]/([Cs^+] + [Li^+])$). (*a*) Current–voltage (*I–V*) relationships for one patch for $X_{Cs} = 1$ (filled circles), $X_{Cs} = 0.6$ (empty circles) and $X_{Cs} = 0$ (filled triangles). (*b*,*c*) Normalized mean chord conductances, G_{norm}, between ± 60 mV and V_{rev}, plotted against X_{Cs}; (*b*) $+60$ mV, (*c*) -60 mV ($n = 3$). At both potentials, larger conductances were present when $X_{Cs} = 0.6$ compared to pure Cs^+ or Li^+ solutions. (*d*) Single-channel current–voltage (*I–V*) curves with decreasing X_{Cs} on the cytoplasmic side ($X_{Cs} = 1$ (filled circles), $X_{Cs} = 0.6$ (empty circles) and $X_{Cs} = 0$ (filled squares)). (*e*,*f*) Normalized mean single-channel chord conductances, γ_{norm}, between ± 60 mV and V_{rev}; (*e*) $+60$ mV, (*f*) -60 mV (n =3). Single-channel results showed clear AMFE at positive membrane potentials only. Error bars indicate s.e.m.

pure solution alone, indicating AMFE. At negative membrane potentials, unitary currents in the presence of Na^+–NH_4^+ mixtures were intermediate between those in the presence of NH_4^+ alone and those in the presence of Na^+alone. The calculated V_{rev} values were -12.9 ± 2.0 mV ($X_{Na} = 0$), -6.5 ± 1.6 mV ($X_{Na} = 0.8$) and 0.3 ± 0.3 mV ($X_{Na} = 1.0$) ($n = 3$). V_{rev} measured in the NH_4^+ solution shifted to a value substantially more negative than that in the Na^+ solution, indicating that rOCNC1 channels are more permeable to NH_4^+ than to Na^+, as we have reported previously (Qu *et al*. 2000). The plot of V_{rev} against the mole fraction of Na^+ shows a monotonic relationship without any AMFE (results not shown). The normalized chord conductances between $+60$ mV and V_{rev} were 1.05 ± 0.02 ($X_{Na} = 0$), 0.8 ± 0.03 ($X_{Na} = 0.8$) and 1.0 ($X_{Na} = 1.0$) ($n = 3$), while the corresponding values between V_{rev} and -60 mV in the same three patches were 1.09 ± 0.02 ($X_{Na} = 0$), 1.03 ± 0.01 ($X_{Na} = 0.8$) and 1.0 ($X_{Na} = 1.0$). The results show that at a membrane potential of $+60$ mV, the normalized chord conductance for $X_{Na} = 0.8$ was significantly lower than those for the pure Na^+ or NH_4^+ solutions ($p < 0.05$), indicating a clear AMFE (figure 2*d*). However, at -60 mV, as the mole fraction of NH_4^+ increased, the normalized chord conductance obeyed a simple monotonic function without any AMFE (figure 2*e*).

In summary, for rOCNC1 channels in mixtures of Na^+–NH_4^+, macroscopic currents exhibited an obvious anomalous drop in conductance at ± 60 mV. However, for single-channel recordings, AMFE were only seen at positive potentials ($+60$ mV), when the ion movement was from the solution mixture. In contrast, at -60 mV, the normalized single-channel conductance decreased monotonically as the mole fraction of Na^+ increased.

Since AMFE have been reported in rod cGMP-gated channels in the presence of two different-sized ions, such as the large polarizable Cs^+ and the small Li^+ (Sesti *et al*. 1995), we tested the effect of mixtures of those two cations in the cytoplasmic solution on our recombinant olfactory CNG channels, again with the total concentration ($[Cs^+] + [Li^+]$) held constant at 145 mM. Figure 3*a* shows the data for currents elicited by 500 μM cAMP for

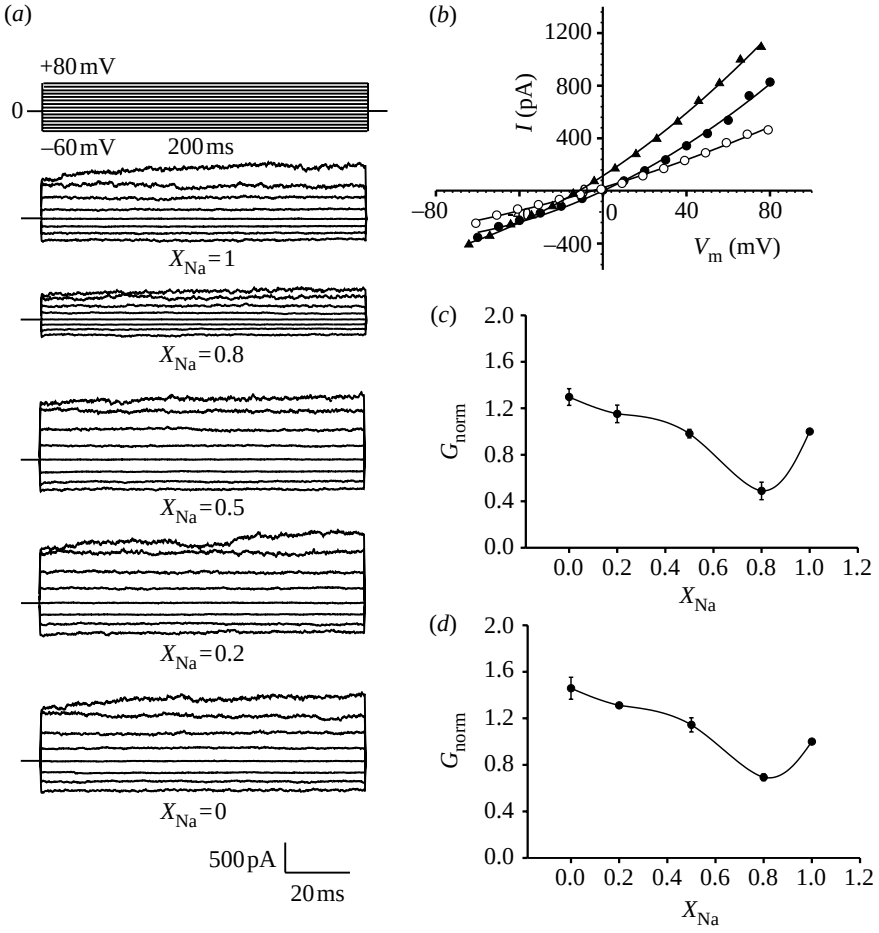

Figure 4. Macroscopic currents through native rat olfactory CNG channels in Na^+–NH_4^+ mixtures; mole fraction, $X_{Na} = [Na^+]/([Na^+] + [NH_4^+])$. (*a*) Representative macroscopic currents in a single inside-out patch from an olfactory-receptor-neuron dendritic knob for different X_{Na}. Currents were elicited by 100 μM cAMP and every second response to the 200 ms voltage protocol (illustrated in the top panel) is displayed. Linear leakage current has been subtracted from each recording and the small bar to the left of each set of current traces indicates the zero-voltage trace. (*b*) Current–voltage (*I–V*) relationships determined in the same patch with decreasing X_{Na} on the cytoplasmic side ($X_{Na} = 1$ (filled circles), $X_{Na} = 0.8$ (empty circles) and $X_{Na} = 0$ (filled triangles)). Minimum currents were obtained for $X_{Na} = 0.8$ at both potentials. (*c*,*d*) Normalized mean chord conductances, G_{norm}, for V_m between ±60 mV and V_{rev}; (*c*) +60 mV, (*d*) −60 mV ($n = 3$). The chord conductance displayed AMFE with a minimum value when $X_{Na} = 0.8$ at both potentials. Error bars represent s.e.m.

different mole fractions of Cs^+, X_{Cs}. The pipette solution, to which the external surface of the membrane patch was exposed, was kept constant and contained 145 mM CsCl. The *I–V* relations obtained in the presence of 145 mM Li^+ ($X_{Cs} = 0$), 87 mM Cs^+ and 58 mM Li^+ ($X_{Cs} = 0.6$) and 145 mM Cs^+ ($X_{Cs} = 1$) in the perfused solutions are shown in figure 3*a*. It can be clearly seen that the currents carried by the Cs^+–Li^+ mixtures (empty circles) were larger than those recorded in either pure ionic solution. The V_{rev} values were -5.5 ± 0.3 mV ($X_{Cs} = 0.0$), -7.5 ± 0.8 mV ($X_{Cs} = 0.6$) and 0.2 ± 0.4 mV ($X_{Cs} = 1$) ($n = 3$) indicating that the V_{rev} obtained for $X_{Cs} = 0.6$ was anomalously more negative than the values measured in either the pure Cs^+ or pure Li^+ solutions. The normalized chord conductances for membrane potentials of +60 mV, relative to the pure Cs^+ value, were 1.2 ± 0.06 ($X_{Cs} = 0$), 1.7 ± 0.05 ($X_{Cs} = 0.6$) and 1.0 ($X_{Cs} = 1$) ($n = 4$), while the corresponding values at −60 mV in the same four patches were 1.04 ± 0.02 ($X_{Cs} = 0$), 1.5 ± 0.11 ($X_{Cs} = 0.6$) and 1.0 ($X_{Cs} = 1$); thus, we observed classic anomalous mole-fraction behaviour in that the normalized conductance of the Cs^+–Li^+ mixture was significantly larger than that in either the pure Cs^+ or the pure Li^+ solutions at both positive and negative potentials ($p < 0.05$, figure 3*b*,*c*).

Single-channel currents evoked by 200 μM cAMP were also measured in three intracellular solution mixtures, $X_{Cs} = 0$, 0.6 and 1.0, as shown in figure 3*d–f*. When the patch pipette was filled with 145 mM Cs^+ and either 145 mM Li^+ or 145 mM Cs^+ was in the bathing medium, the mean reversal potentials (V_{rev}) calculated from the corresponding *I–V* curves in the experiments for three cells (figure 3*d*) were -5.2 ± 0.8 mV ($X_{Cs} = 0$) and 0.3 ± 0.7 mV ($X_{Cs} = 1$), respectively. For $X_{Cs} = 0.6$, V_{rev} shifted non-monotonically to a more negative value, *ca.* -8.8 ± 1.0. The normalized chord conductances for a membrane potential of +60 mV were 1.2 ± 0.01 ($X_{Cs} = 0$), 1.3 ± 0.05 ($X_{Cs} = 0.6$) and 1.0 ($X_{Cs} = 1$) ($n = 3$) ($p < 0.05$, figure 3*e*), thus displaying AMFE for outward currents,

where ion movement is from the solution mixture into the channel. In contrast, at −60 mV in the same three patches the conductances were 0.6 ± 0.03 ($X_{Cs}=0$), 0.9 ± 0.03 ($X_{Cs}=0.6$) and 1.0 ($X_{Cs}=1$), increasing monotonically with the mole fraction of Cs^+ (figure 3*f*) and showing no AMFE.

In summary, for these rOCNCl channels in mixtures of Cs^+–Li^+, macroscopic currents exhibited AMFE with an obvious anomalous increase in conductance at ±60 mV whereas single-channel recordings only exhibited AMFE at positive potentials. In addition, with these ions, V_{rev} exhibited AMFE for both macroscopic and single-channel currents.

(b) *Anomalous mole-fraction experiments in native rat olfactory CNG channels*

Following the observations of anomalous mole-fraction behaviour in the wild-type rOCNCl channel in the presence of mixtures of Na^+–NH_4^+ or Cs^+–Li^+, we also tested the effect of Na^+–NH_4^+ mixtures on native CNG channels, measuring macroscopic cAMP-activated currents across inside-out patches from acutely isolated rat ORNs. In ORNs, most of the CNG channels are located in the dendritic knob and cilia, and only about 7% are present in the soma (Zagotta & Siegelbaum 1996). However, the extremely small size of rat ORNs makes tight-seal recordings (5–10 GΩ) from the dendritic knob difficult. Good current responses were obtained in only three patches, one from the knob and two from the soma. Macroscopic currents were activated by 100 μM cAMP in response to voltage pulses of *ca.* 200 ms duration, ranging from −60 mV to +80 mV in 10 mV steps.

Figure 4*a* shows representative macroscopic currents measured in different mole fractions of Na^+. These CNG channels are highly permeable to both Na^+ and NH_4^+ ions, with larger currents being elicited in pure NH_4^+ solution than in pure Na^+ solution. As observed in the recombinant CNG channels, the current amplitudes went through a distinct minimum for both positive and negative potentials at $X_{Na}=0.8$ (figure 4*c*,*d*). The mean V_{rev} values, calculated from the interpolation of the I–V curves (figure 4*b*) were −8.3 ± 0.9 mV ($X_{Na}=0.0$), −4.5 ± 0.8 mV ($X_{Na}=0.8$) and −0.3 ± 0.3 mV ($X_{Na}=1.0$) ($n=3$), showing only a simple monotonic increase as the Na^+ mole fraction increased. However, the normalized chord conductances at a membrane potential of +60 mV were 1.3 ± 0.079 ($X_{Na}=0.0$), 0.5 ± 0.08 ($X_{Na}=0.8$) and 1.0 ($X_{Na}=1.0$) ($n=3$, figure 4*c*), while the corresponding values at −60 mV in the same three patches were 1.5 ± 0.09 ($X_{Na}=0.0$), 0.7 ± 0.03 ($X_{Na}=0.8$) and 1.0 ($X_{Na}=1.0$) (figure 4*d*).

Thus, macroscopic currents in native rat olfactory CNG channels also went through a minimum at a mole fraction of *ca.* 0.8 for both positive and negative potentials, markedly similar to the results obtained in wild-type rOCNCl channels in HEK 293 cells.

4. DISCUSSION

This paper presents the first evidence known to the authors for AMFE in recombinant wild-type α-homomeric rat olfactory CNG (rOCNCl) channels expressed in HEK 293 cells, with Na^+–NH_4^+ or Cs^+–Li^+ mixtures, and for native rat olfactory CNG channels in Na^+–NH_4^+ mixtures. Basing our interpretation on the most-accepted mechanisms underlying AMFE, these results imply a multi-occupancy nature of the channels and suggest that at least two ions can concurrently occupy the pore of both native CNG and wild-type rOCNCl channels. The results also show some potential-dependent differences in AMFE between single-channel and macroscopic measurements, suggesting that the molecular basis for AMFE lies within the transmembrane field. This work, together with that in a recent paper (Qu *et al.* 2000), also supports the idea that the rOCNCl channel should be a useful model for structure–function studies of permeation and ionic interaction within the CNG channel.

As previously discussed (§ 1), AMFE in the presence of certain pairs of permeating ions is defined as a deviation from a simple monotonically increasing or decreasing function of conductance (or relative permeability) with mole fraction of one of the constituents (e.g. Hille 1992). Hence, the channel conductance measured in the presence of a mixture of both ions can be significantly larger or smaller than that found in either pure ionic solution alone. AMFE can also be investigated by monitoring parameters such as reversal potentials and permeability ratios and can provide important evidence for ion interaction, which needs to be taken into account in models of ion permeation through ionic channels (e.g. Hille 1992).

Various alternative models have been suggested to account for AMFE, including an electrodynamic model for permeation that suggests that the effects can occur in the absence of multiple binding sites within the pore (Nonner *et al.* 1998). Another possible explanation is that there is an external regulatory site that controls permeation through the pore region (Hille & Schwarz 1978). However, the most widely accepted explanation is that AMFE occur because of multiple-ion occupancy of the pores. The broad underlying principle is that for a certain mole fraction of two critical ion species, both ion types will have an equal probability of being present concurrently within a region of the channel and that their simultaneous presence could result, in terms of rate-theory models of permeation, in either an increase in the depth of a rate-limiting energy well in the channel (giving rise to a concomitant decrease in the channel conductance) or a reduction in the depth of the energy well (giving rise to a concomitant increase in the channel conductance). More recent reports using site-directed mutagenesis have suggested a modification of this model in which it is proposed that permeability and selectivity in multi-ion pores are governed by two or more binding sites of differing affinity (for a review see Lester & Dougherty 1998). Although many theoretical schemes have been described, the precise mechanism underlying the effect is not known and its adequate elucidation probably requires combined structure–function molecular biological and patch-clamp approaches, together with theoretical electrodynamic analyses.

However, it should be noted that this effect has only been demonstrated with certain pairs of ions (e.g. K^+–Tl^+ (Hagiwara *et al.* 1977), Ba^{2+}–Ca^{2+} and Na^+–Ca^{2+} (Almers & McCleskey 1984), K^+–NH_4^+, K^+–Rb^+ and K^+–Tl^+ (Wagoner & Oxford 1987), Na^+–NH_4^+ (Furman & Tanaka 1990) and Li^+–Cs^+ (Sesti *et al.* 1995)), that it is

more likely to occur when one of the ions is large and polarizable (Hille & Schwarz 1978) and that it also depends on the structure of, and ionic interactions in, the particular channel. For example, in the case of native cGMP-gated channels in salamander rod outer segments, although no AMFE were observed in the presence of Li^+–Na^+ mixtures (Menini 1990) or Ca^{2+}–Na^+ mixtures (Zimmerman & Baylor 1992), a clear AMFE was demonstrated in Li^+–Cs^+ mixtures (Sesti *et al*. 1995). Similarly, although conductance measurements in native olfactory CNG channels in rats and frogs showed no AMFE for Na^+–Li^+ mixtures (Frings *et al*. 1992), we have now shown AMFE in both Na^+–NH_4^+ mixtures (with a conductance minimum at $X_{Na} = 0.8$ in both native rat CNG channels and α-homomeric recombinant rat CNG channels) and Cs^+–Li^+ mixtures (with a maximum for the recombinant channels at $X_{Cs} = 0.6$).

Our results show, for the recombinant α-homomeric wild-type rOCNCl channels and native rat CNG channels in Na^+–NH_4^+ mixtures, that an X_{Na} of 0.8 resulted in a conductance minimum for macroscopic currents at both positive and negative potentials. Presumably, with the concurrent presence of Na^+ and NH_4^+ in a region of the channel, the energy wells within the pore become even deeper, possibly as a result of induced dipole effects between Na^+ and NH_4^+, with a resultant decrease in ion–ion repulsion inside the multiply-occupied pores and a reduction in the velocity with which the ions pass through the pore. Unlike the macroscopic case, single-channel currents through the recombinant CNG channels in Na^+–NH_4^+ mixtures only produced a conductance minimum at positive potentials, when the currents would be going from the solution mixture to the channel. This would immediately argue against any simple extracellular regulatory-site model, since such a model would not be expected to be voltage dependent. The macroscopic results also suggest that there is an additional gating-component effect, which occurs independently of current direction. While we did not undertake any long single-channel recordings, some of our results suggested that there was an anomalous decrease in open probability in Na^+–NH_4^+ mixtures in support of a gating effect (e.g. figure 2*a*). These results demonstrate that additional information can be gained by measuring both macroscopic and single-channel properties to distinguish between the effects on permeation and gating. In addition, we did not observe any AMFE on V_{rev} in Na^+–NH_4^+ mixtures. The absence of such effects has also been noted for the Shaker H4 channel, which displays AMFE for single-channel conductance but not for reversal potentials (Heginbotham & MacKinnon 1993).

In our experiments with recombinant channels in Cs^+–Li^+ mixtures, AMFE were observed at $X_{Cs} = 0.6$. However, for this ion pair there was a larger channel conductance at this mole fraction than in pure Cs^+ and Li^+ solutions. Similar results have been reported with Cs^+–Li^+ mixtures in rod cGMP-gated channels (Sesti *et al*. 1995). Both Cs^+ and Li^+ ions are less permeable than Na^+ in rOCNCl channels (Qu *et al*. 2000), although Frings *et al*. (1992) suggested that CNG channels have high-affinity binding sites for Cs^+ and Li^+ ions. Presumably, with the concurrent presence of Cs^+ and Li^+ within the channel, the deep energy wells of the pore are made shallower, possibly by an increase in ion–ion repulsion inside multiply occupied pores, thus enabling the ions to pass through more rapidly, despite possible high-affinity binding sites within the channel. The reversal potential (V_{rev}) of the recombinant channel in these solutions also demonstrated AMFE, further supporting a multi-ion nature for the channel, since V_{rev} does not depend on the number of open channels and should not be affected by channel gating. Again, there were some differences at the single-channel level, with AMFE being observed only for outward currents.

Further studies still need to be performed to analyse the molecular basis of the multi-ion nature of the CNG channel. It has been reported that in both CNG and Ca^{2+} channels the coordination of the negatively charged glutamates in repeats I–IV constitutes a binding site that can be occupied by one or two small ions and provides the molecular structure underlying the high turnover rate necessary for physiological ion permeation (e.g. Sesti *et al*. 1995). Since the amino-acid sequence of the wild-type rOCNCl channel is known (Dhallan *et al*. 1990), it should be possible to identify which amino acids can alter ionic selectivity, abolish AMFE and contribute to the multi-ion nature of the pore. The most likely candidate is the glutamate residue in the pore region of each of the four subunits. Indeed, Sesti *et al*. (1995) reported that mutations in this residue in the rod cGMP-gated channel abolished AMFE. In combination with site-directed mutagenesis (especially in the P-domain), AMFE behaviour should provide useful information about the structural and functional relationships of the permeation pathway of the CNG channels.

We acknowledge the support of the Australian Research Council, the National Health and Medical Research Council of Australia and the Garnett Passe and Rodney Williams Memorial Foundation. We thank Dr Stephan Bieri for provision of the recombinant rOCNCl CNG channels in HEK 293 cells and Ms Irene Michas and Anna Scimone for maintenance of the HEK 293 cells.

REFERENCES

Almers, W. & McCleskey, E. W. 1984 Non-selective conductance in calcium channels of frog muscle, calcium selectivity in a single-file pore. *J. Physiol.* (*Lond.*) **353**, 585–608.

Barry, P. H. 1994 JPCalc, a software package for calculating liquid junction potential corrections in patch-clamp, intracellular, epithelial and bilayer measurements and for correcting liquid junction potential measurements. *J. Neurosci. Meth.* **51**, 107–116.

Bradley, J., Li, J., Davidson, N., Lester, H. A. & Zinn, K. 1994 Heteromeric olfactory cyclic nucleotide-gated channels: a subunit that confers increased sensitivity to cAMP. *Proc. Natl Acad. Sci. USA* **91**, 8890–8894.

Chen, C. & Okayama, H. 1987 High efficiency expression of mammalian cells by plasmid DNA. *Mol. Cell Biol.* **7**, 2745–2751.

Dhallan, R. S., Yau, K-W., Schrader, K. A. & Reed, R. R. 1990 Primary structure and functional expression of a cyclic nucleotide-activated channel from olfactory neurons. *Nature* **347**, 184–187.

Frings, S., Lynch, J. W. & Lindemann, B. 1992 Properties of cyclic nucleotide-gated channels mediating olfactory transduction. *J. Gen. Physiol.* **100**, 45–67.

Furman, R. E. & Tanaka, J. C. 1990 Monovalent selectivity of the cyclic guanosine monophosphate-activated ion channel. *J. Gen. Physiol.* **96**, 57–82.

Hagiwara, S., Miyazaki, S., Krasne, S. & Ciani, S. 1977 Anomalous permeabilities of the egg cell membrane of a starfish in K^+–Tl^+ mixtures. *J. Gen. Physiol.* **70**, 269–281.

Heginbotham, L. & MacKinnon, R. 1993 Conduction properties of the cloned Shaker K^+ channel. *Biophys. J.* **76**, 2089–2096.

Hille, B. 1992 *Ionic channels of excitable membranes*, 2nd edn. Sunderland, MA: Sinauer Associates.

Hille, E. & Schwarz, W. 1978 Potassium channels as multi-ion single-file pores. *J. Gen. Physiol.* **72**, 409–442.

Lester, H. A. & Dougherty, D. A. 1998 New views of multi-ion channels. *J. Gen. Physiol.* **111**, 181–183.

Lynch, J. W. & Barry, P. H. 1989 Action potentials initiated by single channel openings in a small neuron (rat olfactory receptor). *Biophys. J.* **55**, 755–768.

Menini, A. 1990 Currents carried by monovalent cations through cyclic GMP-activated channels in excised patches from salamander rods. *J. Physiol.* **424**, 167–185.

Nonner, W., Chen, D. P. & Eisenberg, B. 1998 Anomalous mole fraction effect, electrostatics and binding in ionic channels. *Biophys. J.* **74**, 2327–2334.

Qu, W., Zhu, X. O., Moorhouse, A. J., Bieri, S., Cunningham, A. M. & Barry, P. H. 2000 Ion permeation and selectivity of wild-type recombinant rat CNG (rOCNC1) channels expressed in HEK293 cells. *J. Membrane Biol.* **178**, 137–150.

Rispoli, G. & Detwiler, P. B. 1990 Nucleoside triphosphates modulate the light-regulated channel in detached rod outer segments. *Biophys. J.* **57**, 368A.

Sesti, F., Eismann, E., Kaupp, U. B., Nizzari, M. & Torre, V. 1995 The multi-ion nature of the cGMP-gated channel from vertebrate rods. *J. Physiol.* **487**, 17–36.

Wagoner, P. K. & Oxford, G. S. 1987 Cation permeation through the voltage-dependent potassium channel in the squid axon. Characteristics and mechanisms. *J. Gen. Physiol.* **90**, 261–290.

Zagotta, W. N. & Siegelbaum, S. A. 1996 Structure and function of cyclic nucleotide-gated channels. *A. Rev. Neurosci.* **19**, 235–263.

Zimmerman, A. L. & Baylor, D. A. 1992 Cation interactions within the cyclic GMP-activated channel of retinal rods from the tiger salamander. *J. Physiol.* **449**, 759–783.